

I. THE IMMUNOHISTOCHEMICAL STUDY: TOPOGRAPHY OF THE CARDIAC NERVE PLEXUS ON THE RABBIT HEART BASE

Ligita Gukauskienė

Institute of Anatomy, Faculty of Medicine, Lithuanian University of Health Sciences

A. Mickevičiaus 9, Kaunas LT-44307, Lithuania

e-mail: ligitagu123@gmail.com; Phone: +370 37 327218; Mobile: + 370 658 77545

Abstract. The purpose of this study was to investigate the neurotopography of the cardiac ganglionated nerve plexus in the whole-mount preparations of the rabbit atria, because the intrinsic cardiac nervous system of the rabbit has not been investigated so far. The cardiac nerve structures were revealed by the immunofluorescence labelling for the general neuronal marker PGP 9.5 and the substance P (SP) in whole-mount atrial preparations derived from 8 young rabbits. The majority of rabbit intrinsic cardiac neurons (ICNs) were concentrated within three large ganglia containing up to several hundred neurons. In all examined hearts, the total number of the ICNs ranged from 1254 to 2614. The differences between the average of the neuron number of the right and left ganglion clusters were statistically significant at $P < 0.05$. The ganglia interconnected by commissural nerves into the continuous ganglionated nerve plexus on the heart base that encircled the roots of the pulmonary veins (PVs). The somata of the ICNs displayed the immunoreactivity for PGP 9.5. The SP was not observed in the somata of the ICNs. The SP-IR fibres with varicose nerve terminals passed closely to the ICNs but never formed the pericellular baskets around the neuronal somata. The extrinsic cardiac nerves entered the heart base were at the bifurcation of the pulmonary trunk and spread in the left atrium as well as proceeded on the heart base toward the large intrinsic ganglia and on the epicardium towards the root of the right cranial vein (RCV). The SP-IR nerve fibres with numerous varicosities were abundant within nerve bundles. In conclusion, the topography of the cardiac nerve ganglionated plexus of the rabbit heart base corresponds rather well to the rat and the mouse.

Keywords: intrinsic cardiac neurons, rabbit, PGP 9.5, cardiac nerves, substance P

Introduction. Physiological studies have showed that the coronary blood flow as well as cardiac functions, i.e. chronotropic, dromotropic and inotropic, are influenced by intrinsic cardiac ganglionated plexus that contains a heterogeneous population of neural elements including preganglionic and postganglionic nerve fibres, and cardiac ganglia containing parasympathetic, sympathetic, afferent and local circuit neurons with a wide range of neurotransmitter phenotypes (Thompson et al., 2000; Randall et al., 2003; Hoover et al., 2008). In contrast to the hearts of other mammalian species, the neurotopography of the rabbit intrinsic cardiac nerve ganglionated plexus has been poorly examined. Physiological studies have shown that tachykinins such as substance P (SP) influence the ICNs and have suggested that afferent neurons also play a modulatory role within the cardiac ganglia (Hardwick et al., 1995; Thompson et al., 1998). Experiments in isolated cultured ICNs demonstrate that SP can inhibit acetylcholine induced currents through nicotinic receptors (Cuevas and Adams, 2000). Perhaps the SP-immunoreactive nerve fibres that innervate the ICNs represent collateral branches of nociceptive neurons and SP might be released in the intrinsic cardiac ganglia through an axon reflex triggered by myocardial ischemia (Hoover et al., 2000; Hoover et al., 2008).

Therefore, the aim of the present study was two-fold 1) to examine the topography of the rabbit intrinsic cardiac nerve plexus revealed immunohistochemically for PGP 9.5, and 2) to identify the distribution of SP-immunoreactive nerve fibres within the whole mount preparations of the rabbit atria. This is the first

immunohistochemical investigation of the rabbit intrinsic cardiac nerve ganglionated plexus performed in whole mount preparations of the rabbit atria using immunofluorescence labelling for PGP 9.5 and SP.

Materials and Methods. Eight White New Zealand rabbits of both sexes (4–6 weeks old and weighing 0.658 ± 0.093 kg) were used in the present study. The animals were anesthetized with a lethal dose of sodium thiopental (30 mg/kg i.v.) in accordance with local and state guidelines for the care and use of laboratory animals (Permission No. 0206).

Whole mount preparation. To examine the intrinsic cardiac neural plexus using immunofluorescence, hearts perfused with 0.01 M phosphate-buffered saline (PBS; 0.9% NaCl, pH 7.4) were removed from the chest and placed into a dissecting dish containing cold 0.01 M PBS as described previously (Rysevaite et al., 2011). For optimal visualization of neural structures, the atrial walls were separated from the ventricles and then pinned on a silicone pad in a dissecting dish, in which tissues were prefixed for 45 min at 4 °C in a 4% paraformaldehyde solution in 0.01 M phosphate buffer (pH 7.4). To decrease the background light during fluorescence microscopy, the tissues were cleared using a dimethylsulfoxide and hydrogen peroxide solution and dehydrated as reported previously (Dickie et al., 2006). After tissue clearing, the whole-mount preparations were rehydrated by successive 15-minute washes through a graded ethanol series, then washed, and permeabilized in 3 x 10-minute changes of 0.01 M PBS containing 0.5% Triton X-100 (Carl Roth, Karlsruhe, Germany). Nonspecific binding was blocked

for 2 h in PBS containing 5% normal donkey serum (Jackson ImmunoResearch Laboratories, West Grove, PA, USA) and 0.5% Triton X-100. Next, preparations were washed three times for 10 min in 0.01 M PBS and incubated in a mixture of double primary antibodies for 48 h in a dark humid chamber at +4 °C (table 1). After three 10 min-washes in 0.01 M PBS, the whole-mount heart preparations were incubated in an appropriate combination of secondary antibodies for 4 h in a dark

humid chamber on a shaker stage at room temperature (Table 1). All antibodies were diluted in 0.01 M PBS. Thereafter the specimens were again washed in 0.01 M PBS, incubated for 2 h in a dimethylsulfoxide and PBS mixture, 1:4 (v:v) ratio, and mounted in Vectashield Mounting Medium (Vector Laboratories, California, USA). A cover slip was placed on the tissue and then sealed with clear nail polish. Both positive and negative controls were used.

Table 1. Primary and secondary antisera used in the study

Antigen	Host	Dilution	Supplier	Catalogue number
Primary				
ChAT	Goat	1:100	Chemicon ^a	AB 144P
SP	Guinea pig	1:1000	Abcam ^{ab}	ab 10353
PGP 9.5	Mouse	1:200	Nordic BioSite ^c	7863-1004
Secondary				
Mouse ^{FITC}	Donkey	1:100	ImmunoStar ^d	715-095-151
Goat ^{Cy3}	Donkey	1:300	Chemicon ^a	AP 180C
Guinea pig ^{FITC}	Donkey	1:500	Sigma-Aldrich ^e	CF TM 488A
^a Chemicon International, Temecula, California, USA; ^b Abcam plc., Cambridge, UK; ^c Nordic BioSite ^c , By Your Side TM In Life Science Research, Täby, Sweden; ^d ImmunoStar Incorporation, Wisconsin, USA; Jackson ImmunoResearch Europe Ltd., Suffolk, UK; ^e Sigma-Aldrich, St. Louis, MO, USA				

Microscopic examination and quantitative analysis. Whole-mount preparations stained immunohistochemically were analyzed utilizing an AxioImager Z1 fluorescence microscope (Zeiss, Gottingen, Germany) equipped with a set of filters to observe the fluorescein isothiocyanate (FITC) and cyanine (Cy3) fluorescence, an Apotome (Zeiss, Gottingen, Germany), and a digital monochrome camera AxioCam MRm (Zeiss, Gottingen, Germany). The number of neurons inside intrinsic cardiac ganglia was estimated in 0.3-0.5 μ m optical sections of the whole-mount preparations by counting exclusively the PGP 9.5-IR immuno-reactive nerve cells that contained well-visible nuclei. The adjustments of final images and measurements of cardiac neural structures were performed using AxioVision 4.8.1 software (Zeiss, Jena, Germany).

Statistical analysis. Data were processed using the Origin Lab software version 6.1 (OriginLab Corporation, Northampton, MA, USA). The data shown both in the text and graphs are expressed as mean \pm standard error of mean (SEM). Statistical significance of the difference between the means was performed with Student's paired and independent tests. The differences were considered statistically significant at $P < 0.05$.

Results. The locations of the intrinsic cardiac nerve plexus and neural ganglia were visualised in five whole-mount preparations of the rabbit atria (Fig. 1). The general neuronal marker PGP 9.5 was used to identify all ICNs, nerves and nerve bundles (Fig. 1). The double labelling for ChAT and PGP 9.5 showed that the majority of neuronal somata demonstrated the immunoreactivity for ChAT (Fig. 2). On the rabbit heart base, i.e. at the roots of the PVs, three large ganglia containing up to

several hundred ICNs and numerous small additional ganglia involving from 3 to 50 ICNs were found (Fig. 1). Both the number and the size of ganglia varied from rabbit to rabbit. The individual ICNs were observed on the rabbit heart base, along the nerves and nerve bundles (Fig. 2). For practical reasons, the rabbit intrinsic cardiac ganglia were divided into the right (RC) and the left clusters (LC) as determined by condition landmarks (Table 2; Fig. 1). The RC involved the intrinsic cardiac ganglia and individual ICNs permanently situated between the roots of the RCV and the right pulmonary vein (RPV). The left cluster was composed of the neural ganglia and the separate ICNs that were constantly distributed: (1) between the roots of the caudal cava vein (CV) and the middle pulmonary vein (MPV); (2) between the roots of the left cranial cava vein (LCV) and the left pulmonary vein (LPV); (3) subepicardially beneath the MPV. In all examined preparations, the ICG were interconnected by commissural nerves into the continuous ganglionated nerve plexus on the heart base and this plexus completely encircled the roots of the PVs (Fig. 1).

Table 2. The mean number and the range of the PGP 9.5-IR intrinsic neuronal somata in the five rabbit whole-mount preparations. The differences between the right and the left clusters were statistically significant at $P < 0.05$

Neurons	Mean	Range
Right cluster	637 \pm 53	335 – 923
Left cluster	1119 \pm 143	686 – 1754
Singular	288 \pm 65	164 – 524
In average per atria	1963 \pm 128	1254 – 2614

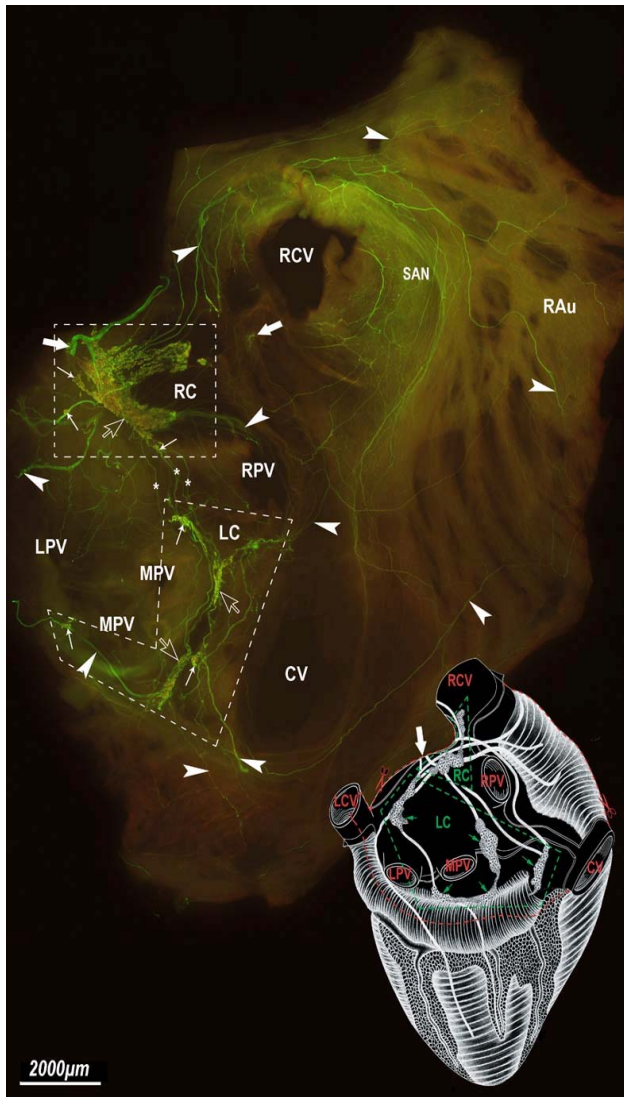


Fig. 1. The whole-mount preparation of the rabbit atria and the schematic drawing of the rabbit heart base in the right lower corner demonstrate the morphology and topography of the ganglionated nerve plexus on the heart base. The whole-mount preparation shows the morphologic pattern of the nerve structures labelled immunohistochemically for protein gene product 9.5 (in green) and choline acetyltransferase (in red). The left cranial cava vein was extirpated in order to flatten the atria. The white dashed polygonal areas point the areas occupied by the right (RC) and the left (LC) clusters of the intrinsic cardiac ganglia; the red dashed line – the boundaries of the flattened atria; the thick white arrows – the extrinsic cardiac nerves entering the ganglionated nerve plexus; the white arrowheads – the nerves extending to the innervation regions; the thin white arrows – the small clusters; open white arrow – the main clusters; asterisks – the commissural nerves communicating distinct ganglia. Abbreviations: CV – caudal vein; LC – left cluster; LCV – left cranial vein; LPV – left pulmonary vein; MPV – middle pulmonary vein; RAu – right auricle; RC – right cluster; RCV – right cranial vein; RPV – right pulmonary vein; SAN – sinoatrial nodal region.

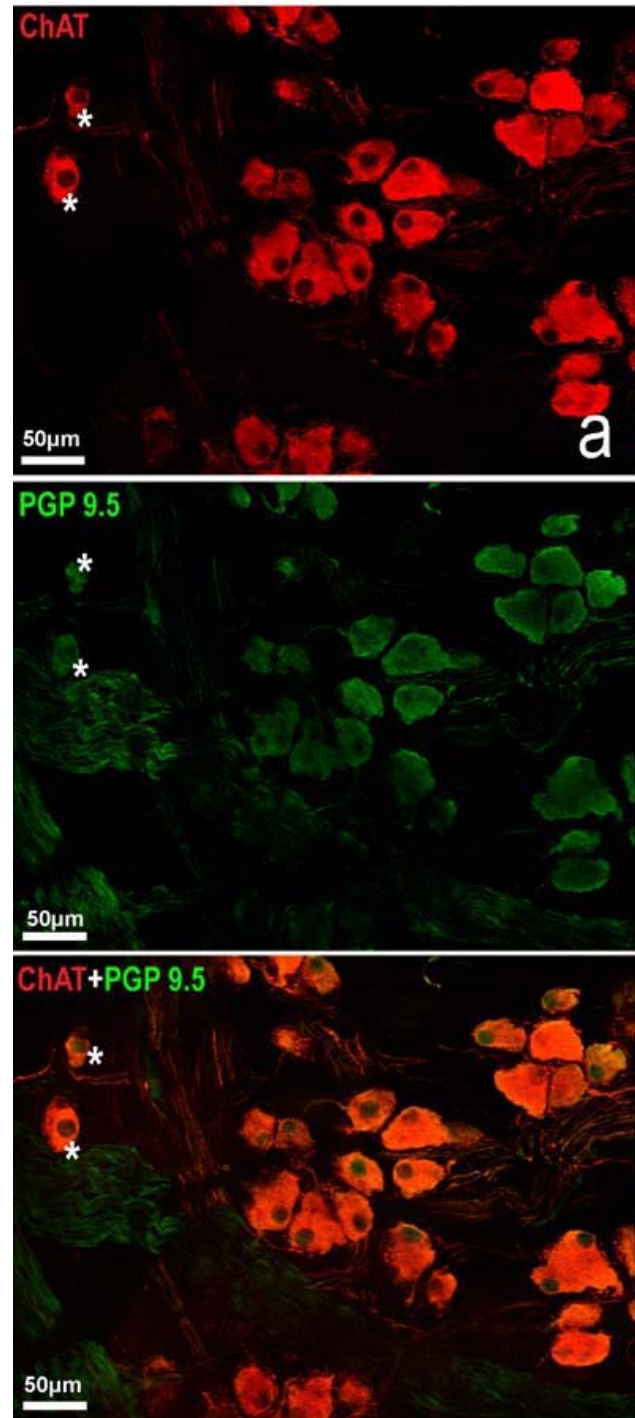


Fig. 2. The microphotograph of the whole-mount preparations of atria demonstrates cardiac neurons immunoreactive for the PGP 9.5 immunoreactive neurons (green) and ChAT (red). The asterisks point the individual neurons located at the nerve bundle

In all examined whole-mounts, the numerous extrinsic cardiac nerves accessed both the RC and the LC of cardiac ganglia between the roots of the RCV and the LCV, i.e. through the fat-pad at the bifurcation of the pulmonary trunk (Fig. 1). The singular and thin extrinsic cardiac nerves constantly entered the right ganglion cluster at the medial side of the root the RCV (Fig. 1). The numerous thin nerves and the nerve bundles branched

from the ganglia of the RC and passed: (1) to sinoatrial nodal (SAN) area, i.e. to the ventral, lateral and dorsal sides of the root of the RCV and between the right auricle and the root of the CV; (2) around the root of the RPV; (3) to the ganglia of the LC (Fig. 1). The nerve branches of the ganglia of the LC extended towards: (1) to the SAN area, i.e. between the roots of the RPV and the CV; (2) around the roots of all PVs; (3) to the ganglia of the right cluster; (4) onto the dorsal wall of both atria (Fig. 1).

The peptidergic nerve structures examined in three whole-mount preparations of the rabbit atria using the antibodies to the substance P (SP). The immunoreactivity for the SP was observed in the numerous varicose nerve fibres but never in the neuronal somata (Fig. 3). The SP-IR nerve fibres were identified within the nerves and the nerve bundles (Fig. 3). In the every ganglion, the SP-IR had numerous varicoses and passed closely to the ICNs but never formed pericellular baskets around the somata of the ICNs (Fig. 3).

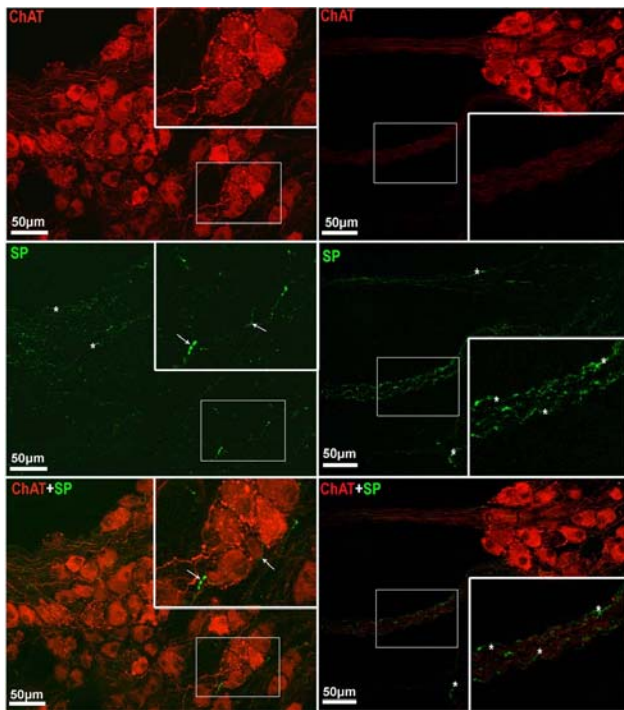


Fig. 3. The microphotographs of the whole-mount atrial preparation double labelled for the ChAT (red) and the SP (green) demonstrating the SP-IR nerve fibres identified within the nerves and the nerve bundles. Note the SP-IR fibres with numerous varicoses passing closely to the ICNs but never forming the pericellular baskets around the somata of the ICNs. Boxed areas are enlarged in the right upper corners to demonstrate the SP-IR varicose nerve fibres. The asterisks point the SP-IR varicose nerve fibres within nerves and nerve bundles, white thin arrows – the SP-IR varicose fibres near the ChAT-IR neurons.

Discussion. The results of this study demonstrate the complex neurochemical morphology of the epicardiac nerve plexus on the rabbit heart base. The whole-mount

preparations of the rabbit atria allowed revealing the distribution of the PGP 9.5 and the peptidergic nerve structures within the non-sectioned epicardiac nerve plexus. In order to prepare the whole-mount preparations of the rabbit atria, 4–6 week old rabbits were used in the present study. The appearance of the cholinergic, adrenergic, and peptidergic intrinsic cardiac nerve structures in the human and mouse fetal hearts during the period of mid-gestation (Gordon et al., 1993; Fregoso and Hoover, 2012) and confirmation of the autonomic regulation of the heart rate in the newborn mice (Sato, 2008), support the use of the rabbits 4–6 weeks old in the present study. The thickness of the atrial wall was substantial even in the hearts of the young rabbits. Therefore our examinations were focused on the epicardiac layer of the intrinsic cardiac nerve plexus which is considered the densest layer compared to the myocardiac or the endocardiac ones (Khabarova, 1975).

In the present study, the immunofluorescence for PGP 9.5 revealed the nerve plexus with the three large neural ganglia containing up to several hundred neurons on the heart base, i.e. at the roots of the PVs. Previous reports have described the topography of the nerve ganglionated plexus in the whole-mount preparations of the guinea pig, rat and mouse atria (Leger et al., 1999; Richardson et al., 2003; Rysevaite et al., 2011). The location and the morphology of the rabbit cardiac ganglia look like in the rat and mouse atria (Richardson et al., 2003; Rysevaite et al., 2011), but are in contrast to the guinea pig atria whose small ganglia consist of 20 neurons (Leger et al., 1999).

The SP-IR nerve fibres with numerous varicosities have been observed in the rabbit intrinsic cardiac ganglia but never formed the pericellular baskets around the neuronal somata. The SP-IR nerve fibres were also identified within the rabbit epicardiac nerves and nerve bundles. The presence of the SP-IR nerve fibres has been previously reported in the rat and mouse ICG (Richardson et al., 2003; Rysevaite et al., 2011). In contrast to the rat intrinsic cardiac ganglia (Richardson et al., 2003), rabbit did not show an extensive network of the SP-IR nerve fibres around the ganglion. The lack of the immunoreactivity for the SP in the vagal nuclei and in the sympathetic postganglionic neurons supports the hypothesis that the SP-IR nerve fibres originated from the afferent neurons of the dorsal root ganglia (Wiesenfeld-Hallin et al., 1984).

A major finding of the present study was that the numerous extrinsic cardiac nerves accessed both the right and the left clusters of cardiac ganglia between the roots of the RCV and the LCV, i.e. through the fat-pad at the bifurcation of the pulmonary trunk. In contrast to the observations in the rat and mouse hearts (Batulevicius et al., 2003; Rysevaite et al., 2011), only single and thin extrinsic rabbit cardiac nerves entered ganglia at the medial side of the root of the RCV, and was not observed entering the nerve at the root of the LCV.

This study provides a detailed neurotopography of the epicardiac nerve ganglionated plexus of the rabbit heart. Our data indicate that (1) the majority of rabbit intrinsic cardiac neurons were concentrated within three large

ganglia containing up to several hundred neurons; (2) the ganglia interconnected by commissural nerves into the continuous ganglionated nerve plexus on the heart base that encircled the roots of the pulmonary veins; (3) the SP-IR nerve fibres with numerous varicosities have been observed in the rabbit intrinsic cardiac ganglia but never formed the pericellular baskets around the neuronal somata; (4) the extrinsic cardiac nerves entered the rabbit heart base at the bifurcation of the pulmonary trunk. In conclusion, the topography of the cardiac nerve ganglionated plexus of the rabbit heart base corresponds rather well to the one of rat and mouse.

Acknowledgements. This study was supported by the Grant of Medical Academy Science Foundation, Lithuanian University of Health Sciences.

References

1. Batulevicius D, Pauziene N, Pauza DH. Topographic morphology and age-related analysis of the neuronal number of the rat intracardiac nerve plexus. *Ann Anat.* 2003. 185(5). P. 449–59.
2. Cuevas J, Adams DJ. Substance P preferentially inhibits large conductance nicotinic ACh receptor channels in rat intracardiac ganglion neurons. *J Neurophysiol.* 2000. 84. P. 1961–1970.
3. Dickie R, Bachoo RM, Rupnick MA, Dallabrida SM, Deloid GM, Lai J, Depinho RA, Rogers RA. Three-dimensional visualization of microvessel architecture of whole-mount tissue by confocal microscopy. *Microvasc Res.* 2006. 72(1–2). P. 20–6.
4. Fregoso SP, Hoover DB. Development of cardiac parasympathetic neurons, glial cells, and regional cholinergic innervation of the mouse heart. *Neuroscience.* 2012. 221. P. 28–36.
5. Gordon L, Polak JM, Moscoso GJ, Smith A, Kuhn DM, Wharton J. Development of the peptidergic innervation of human heart. *J Anat.* 1993. 183. Pt 1. 131–140.
6. Hardwick JC, Mawe GM, Parsons RL. Evidence for afferent fiber innervation of parasympathetic neurons of the guinea-pig cardiac ganglion. *J Auton Nerv Syst.* 1995. 53. P. 166–174.
7. Hoover DB, Chang Y, Hansock JC, Zhang L. Actions of tachykinins within the heart and their relevance to cardiovascular disease. *Jpn J Pharmacol.* 2000. 84. P. 367–373.
8. Hoover DB, Shepherd AV, Southerland EM., Armour JA, Ardell JL. Neurochemical diversity of afferent neurons that transduce sensory signals from dog ventricular myocardium. *Auton Neurosci.* 2008. 141(1–2). P. 38–45.
9. Khabarova A.Y. Innervation of the Heart and Coronary Vessels. Leningrad: Nauka (in Russian); 1975.
10. Leger J, Croll RP, Smith FM. Regional distribution and extrinsic innervation of intrinsic cardiac neurons in the guinea pig. *J Comp Neurol.* 1999. 404. P. 303–317.
11. Randall DC, Brown DR, McGuirt AS, Thompson GW, Armour JA, Ardell JL. Interactions within the intrinsic cardiac nervous system contribute to chronotropic regulation. *Am J Physiol Regul Integr Comp Physiol.* 2003. 285. P. 1066–75.
12. Richardson RJ, Grkovic I, Anderson CR. Immunohistochemical analysis of intracardiac ganglia of the rat heart. *Cell Tissue Res.* 2003. 314. P. 337–350.
13. Rysevaite K, Saburkina I, Pauziene N, Vaitkevicius R, Noujaim SF, Jalife J, Pauza DH. Immunohistochemical characterization of the intrinsic cardiac neural plexus in whole-mount mouse heart preparations. *Heart Rhythm.* 2011. 8. P. 731–738.
14. Sato S. Quantitative evaluation of ontogenetic change in heart rate and its autonomic regulation in newborn mice with the use of a noninvasive piezoelectric sensor. *Am J Physiol Heart Circ Physiol.* 2008. 294. P. 1708–1715.
15. Thompson GW, Hoover DB, Ardell JL, Armour JA. Canine intrinsic cardiac neurons involved in cardiac regulation possess NK1, NK2, and NK3 receptors. *Am J Physiol.* 1998. 275. P. 1683–1689.
16. Thompson DW, Collier K, Ardell JL, Kember G and Armour JA. Functional interdependence of neurons in a single canine intrinsic cardiac ganglionated plexus. *Journal of Physiology.* 2000. 528. P. 5610–571.
17. Wiesenfeld-Hallin Z, Hökfelt T, Lundberg JM, Forssmann WG, Reinecke M, Tschopp FA, Fischer JA. Immunoreactive calcitonin gene-related peptide and substance P coexist in sensory neurons to the spinal cord and interact in spinal behavioral responses of the rat. *Neurosci Lett.* 1984. 52. P. 199–204.

Received 26 September 2013

Accepted 23 October 2013